Multi-wavelength study of extreme high-energy peaked BL Lac (EHBL) source 1ES 0229+200

Rukaiya Khatoon
Postdoctoral Researcher
North-West University, South Africa
Working with **Prof. Markus Böttcher**

Collaborators:
Jyotishree Hota & Ananta C. Pradhan (NIT Rourkela, India), Ranjeev Misra (IUCAA, India)

Hota, Khatoon+, et al. (2024)
arXiv: *https://arxiv.org/abs/2409.12827*

Overview of Blazar :

➢ Class of AGN for which the relativistic jet is pointed towards the observer.

➢ Blazars include two main categories: **Flat Spectrum Radio Quasars (FSRQs)**, which have strong optical emission lines, and **BL Lacertae objects (BL Lacs)**, which have weak or no optical emission lines.

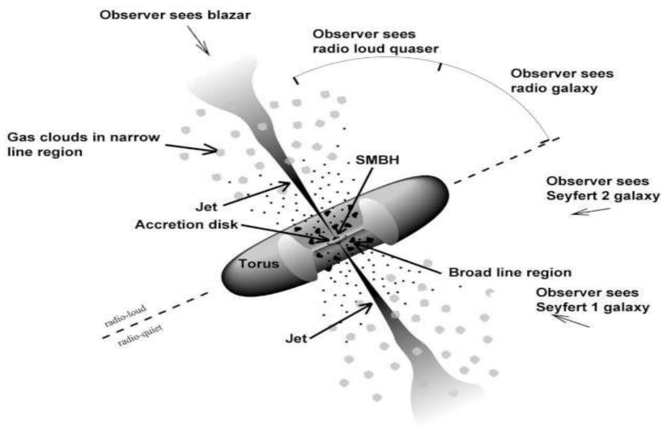

Blazar properties

➢ Non-thermal spectrum extending from radio to GeV/TeV Gamma rays

➢ Rapid variability - both spectral and flux

➢ Typical double hump spectral energy distribution

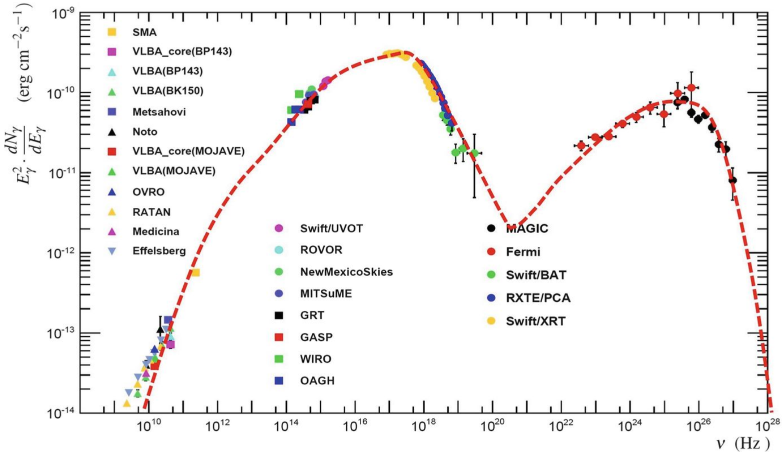

Blazar Sequence :

➔ **Low Synchrotron peaked (LSP/LBL):**

Blazars consisting of FSRQs and LBLs having synchrotron peak frequency < 10^14 Hz

➔ **Intermediate synchrotron peaked (ISP/IBL):**

Blazars classified as BL Lac objects having synchrotron peak frequency 10^14 - 10^15 Hz

➔ **High synchrotron peaked (HSP/HBL):**

Blazars consists of HBLs i.e., BL Lac objects having synchrotron peak frequency > 10^15 Hz

➔ **Extreme high-energy peaked BL Lac objects (EHBLs)**:

For EHBLs, the synchrotron peak located at > 10^17 Hz and a high-energy hump exceeding one TeV.

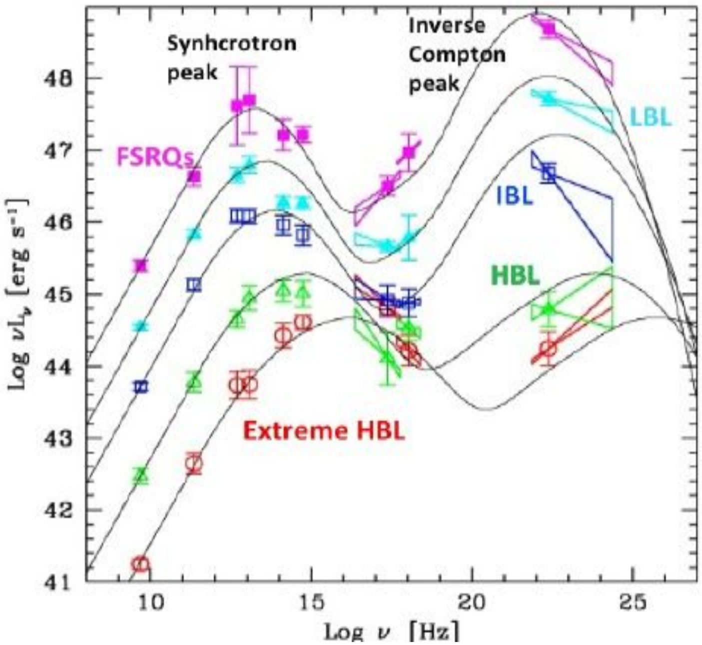

The blazar sequence by Fossati et al. (1998)

Observations of 1ES 0229+200

- 1ES 0229+200 is an EHBL source and is located at redshift z = 0.14. It is classified as hard-TeV blazar because its emission reaches very high-energy gamma rays, with the peak of its SED occurring above some TeV.

- The source was observed over five different epochs between 2017 and 2021 by *AstroSat*, utilizing its onboard instruments: the Ultraviolet Imaging Telescope (UVIT: 130−300 nm), the Soft X-ray Focusing Telescope (SXT: 0.3−8.0 keV), and the Large Area X-ray Proportional Counter (LAXPC: 3−80 keV).

- The Fermi-LAT (100 MeV−300 GeV) data of the source were collected from 2008 to 2022.

- For the VHE γ-ray observations, we used the TeV spectra obtained from the MAGIC observations reported by ***MAGIC Collaboration et al. (2020)***, with a total exposure time of 117.46 hours and spanning a duration from 2013 to 2017.

- We conducted Spectral Energy Distribution (SED) analysis of the source, over different epochs between September 2017 and August 2021.

Details of the AstroSat observations at five epochs:

Observation ID	Instrument	Energy band	Observation date	Exposure (ks)	Count rate (Count/sec)
	LAXPC20	3-30 keV	21-23, Sep 2017	57.4	2.74 ± 0.15
A03_078T01_9000001546	SXT	0.7-7 keV	21-23, Sep 2017	57.4	0.42 ± 0.01
	UVIT	FUVBaF2 (1541 Å)	22, Sep 2017	4.97	0.168 ± 0.007
	UVIT	NUVB13(2447 Å)	22, Sep 2017	5.0	0.463 ± 0.01
	LAXPC20	3-30 keV	9-10, Dec 2017	40	2.99 ± 0.10
A04_130T01_9000001762	SXT	0.7-7 keV	9-10, Dec 2017	40	0.40 ± 0.02
	UVIT	FUVBaF2 (1541 Å)	9, Dec 2017	4.97	0.175 ± 0.006
	UVIT	NUVB13(2447 Å)	9, Dec 2017	4.97	0.468 ± 0.01
	LAXPC20	3-30 keV	21-22, Dec 2017	50	3.15 ± 0.10
A04_130T01_9000001792	SXT	0.7-7 keV	21-22, Dec 2017	50	0.37 ± 0.007
	UVIT	FUVBaF2 (1541 Å)	21, Dec 2017	4.99	0.168 ± 0.006
	UVIT	NUVB13 (2447 Å)	21, Dec 2017	5.0	0.467 ± 0.01
	LAXPC20	3-30 keV	8-9, Dec 2018	57.4	2.52 ± 0.06
A04_130T01_9000001822	SXT	0.7-7 keV	8-9, Jan 2018	57.4	0.42 ± 0.02
	UVIT	FUVBaF2(1541 Å)	8, Jan 2018	4.9	0.175 ± 0.006
	UVIT	NUVB13 (2447 Å)	8, Jan 2018	5	0.50 ± 0.01
	LAXPC20	3-30 keV	8-12, Aug 2021	343.6	2.32 ± 0.09
T04_034T01_9000004632	SXT	0.7-7 keV	8-12, Aug 2021	343.6	0.24 ± 0.006
	UVOT	W1(2600 Å)	8-12, Aug 2021	3	0.613 ± 0.028
	UVOT	W2(1928 Å)	8-12, Aug 2021	3	0.440 ± 0.021
	UVOT	M2(2246 Å)	8-12, Aug 2021	3	0.286 ± 0.015

Modeling the VHE Emission of 1ES 0229+200

➢ Previous Models Explaining VHE Emission:

- **One-zone Leptonic SSC Models:** *Abdo et al. (2011); Aleksic´ et al. (2012); Aliu et al. (2014); Costamante et al. (2018); Xue et al. (2019); Foffano et al. (2019); Diwan et al. (2023) etc.*
- **One-zone Lepto-hadronic Model:** *Zech & Lemoine (2021)*
- **Two-zone Lepto-hadronic Model:** *Aguilar-Ruiz et al. (2022)*

➢ Our Modeling Approach for 1ES 0229+200:

- **Processes:** Synchrotron and Synchrotron Self-Compton (SSC)
- **Particle Distribution Models Applied:**

1. Log-parabola model
2. Broken Power Law model
3. Power Law with a maximum electron energy (γ_{max})
4. Energy-dependent Diffusion (EDD)
5. Energy-dependent Acceleration (EDA)

*Sinha et al. 2017; Goswami et al. 2018; Hota, **Khatoon+**, et al. 2021; **Khatoon** et al. 2022; Bora, **Khatoon+**, et al. 2024*

SED Modeling of 1ES 0229+200

- The synchrotron emissivity due to a relativistic electron distribution n(γ) (***Rybicki & Lightman 1986***) :

$$J_{\rm syn}(\epsilon') = \frac{1}{4\pi}\int P_{\rm syn}(\gamma,\epsilon')\,n(\gamma)\,d\gamma$$

$$P_{\rm syn}(\gamma,\epsilon') = \frac{\sqrt{3}\pi e^3 B}{4 m_e c^2} f\left(\frac{\epsilon'}{\epsilon_c}\right)$$ → *The pitch angle averaged synchrotron power emitted by single particle*

$$\epsilon_c = \frac{3he\gamma^2 B}{16 m_e c}$$

$f\left(\frac{\epsilon'}{\epsilon_c}\right)$ → *The synchrotron power function defined as* → $f(x) = x\int_x^\infty K_{5/3}(\psi)\,d\psi$

$K_{5/3}$ *is the Bessel function of order 5/3*

SED Modeling of 1ES 0229+200

- The synchrotron flux that the observer receives at energy ϵ will be given by (***Begelman, Blandford & Rees 1984***) :

$$F_{\rm syn}(\epsilon) = \frac{\delta^3(1+z)}{d_L^2} V J_{\rm syn}\left(\frac{1+z}{\delta}\epsilon\right)$$
$$= \frac{\delta^3(1+z)}{d_L^2} V \mathbb{A} \int_{\xi_{min}}^{\xi_{max}} f(\epsilon/\xi^2) n(\xi) d\xi$$

$$J_{\rm syn}\left(\frac{1+z}{\delta}\epsilon\right) = \mathbb{A} \int_{\xi_{min}}^{\xi_{max}} f(\epsilon/\xi^2) n(\xi) d\xi$$

Here, the particle energy distribution is expressed by $n(\xi)$, where ξ is represented in such a way that $\xi = \gamma\sqrt{\mathbb{C}}$, where $\mathbb{C} = \frac{\delta}{1+z}\frac{3heB}{16m_e c}$

δ being the jet's Doppler factor, and B is the magnetic field. In the model, the XSPEC “energy” variable is defined as $\xi = \gamma\sqrt{\mathbb{C}}$, where the corresponding observed photon energy is $\epsilon = \xi^2$ (ξ^2 has units of keV).

SED Modeling of 1ES 0229+200

- Local convolution model, $sscicon \otimes n(\xi)$ in XSPEC software package to fit the broadband SED of the source where $n(\xi)$ is the particle distribution.

- **Log parabola (LP):** The underlying particle distribution in this scenario is described as

$$n(\xi) = K(\xi/\xi_r)^{-\alpha-\beta\log(\xi/\xi_r)}$$

Here, particle spectral index is denoted by α at the reference energy $\xi^2 = \xi_r^2$, while β represents the spectral curvature, and $\boldsymbol{K}$ stands for the normalization of the particle density.

- **Broken power-law (BPL):** The particle distribution in this scenario is characterized as

$$n(\xi) = \begin{cases} K(\xi/1\sqrt{keV})^{-p} \text{ for } \xi < \xi_{break} \\ K\xi_{\text{break}}^{q-p}(\xi/1\sqrt{keV})^{-q} \text{ for } \xi > \xi_{break} \end{cases}$$

p and q represent the low and high energy photon indices.

SED Modeling of 1ES 0229+200

❑ **Power-law particle distribution with maximum electron energy (PL with γ_{max}) :**

The steady-state evolution of density is given by **(Kardashev 1962),**

$$\frac{\partial}{\partial\gamma}\left[\left(\frac{\gamma}{\tau_{acc}} - \beta_s\gamma^2\right)n_a\right] + \frac{n_a}{\tau_{esc}} = Q\delta(\gamma - \gamma_0)$$

$$\gamma_{max} = \frac{1}{\beta_s \tau_{acc}}$$

The solution of the steady-state equation,

$$n(\xi) = K\xi^{-p}\left(1 - \frac{\xi}{\xi_{max}}\right)^{(p-2)}$$

$$K = Q_0\tau_a\gamma_0^{p-1}\mathbb{C}^{p/2}, \quad p = \tau_{acc}/\tau_{esc} + 1 \quad , \qquad \xi_{max} = \gamma_{max}\sqrt{\mathbb{C}}$$

The free parameters are, ξ_{max} , p, and the normalization $\mathbb{N}$ defined as,

$$\mathbb{N} = \frac{\delta^3(1+z)}{d_L^2} V\,\mathbb{A}Q_0\tau_{acc}\gamma_0^{p-1}\mathbb{C}^{p/2}$$

SED Modeling of 1ES 0229+200

❑ Energy dependent diffusion model (EDD):

Escape time scale energy dependent or the diffusion coefficient energy is dependent as $\tau_{esc}(\gamma)$ is given by

$$\tau_{esc} = \tau_{esc,R} \left(\frac{\gamma}{\gamma_R} \right)^{-\kappa}$$

The electron energy distribution, $$n(\xi) = K' \xi^{-1} \exp\left[-\frac{\psi}{\kappa} \xi^{\kappa} \right]$$

Where, $$\psi = \eta_R \left(\mathbb{C} \gamma_R^2 \right)^{-\kappa/2} = \eta_R \xi_R^{-\kappa} \qquad \eta_R \equiv \tau_{acc} / \tau_{esc,R}$$

The normalization parameter is given as,

$$\mathbb{N} = \frac{\delta^3 (1+z)}{d_L^2} V \, \mathbb{A} K' \qquad K' = Q_0 \tau_{acc} \sqrt{\mathbb{C}} \exp\left[\frac{\eta_R}{\kappa} \left(\frac{\gamma_0}{\gamma_R} \right)^{\kappa} \right]$$

The free parameters are ψ , k, and the normalization $\mathbb{N}$

❑ Energy dependent acceleration model (EDA):

Escape time scale energy dependent or the diffusion coefficient energy is dependent as $\tau_{acc}(\gamma)$ is given by

$$\tau_{acc} = \tau_{acc,R}\left(\frac{\gamma}{\gamma_R}\right)^{\kappa}$$

The electron energy distribution, $$n(\xi) = K'\xi^{\kappa-1}\exp\left[-\frac{\psi}{\kappa}\xi^{\kappa}\right]$$

Where, $$\psi = \eta_R\left(\mathbb{C}\gamma_R^2\right)^{-\kappa/2} = \eta_R\xi_R^{-\kappa} \qquad \eta_R \equiv \tau_{acc,R}/\tau_{esc}$$

The normalization parameter is given as,

$$\mathbb{N} = \frac{\delta^3(1+z)}{d_L^2}V\mathbb{A}K' \qquad K' = Q_0\tau_{acc,R}\sqrt{\mathbb{C}}\xi_R^{-\kappa}\exp\left[\frac{\eta_R}{\kappa}\left(\frac{\xi_0}{\xi_R}\right)^{\kappa}\right]$$

The free parameters are ψ , k, and the normalization $\mathbb{N}$

SED modeling results for 1ES 0229+200

Model:
Tbabs⊗const⊗sscicon⊗n(ξ)

- **Hydrogen column density (N_H):** 7.9×10^{20} cm^{-2}
- **Size (R):** 10^{17} cm
- **Bulk Lorentz factor (Γ):** 20

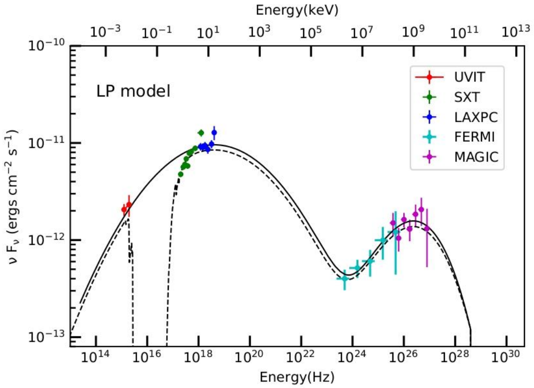

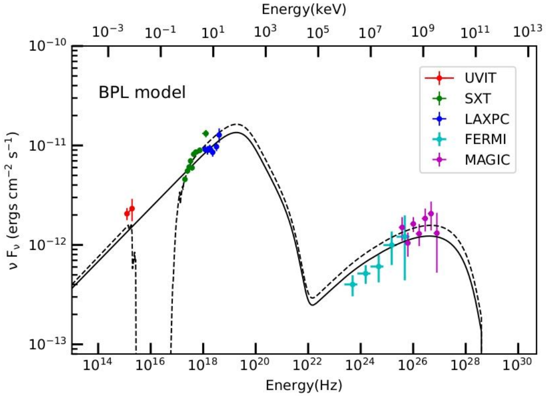

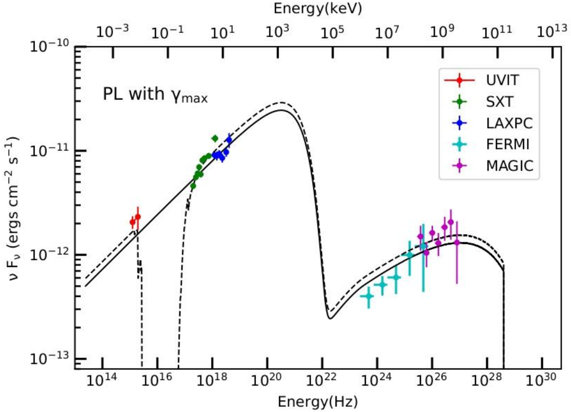

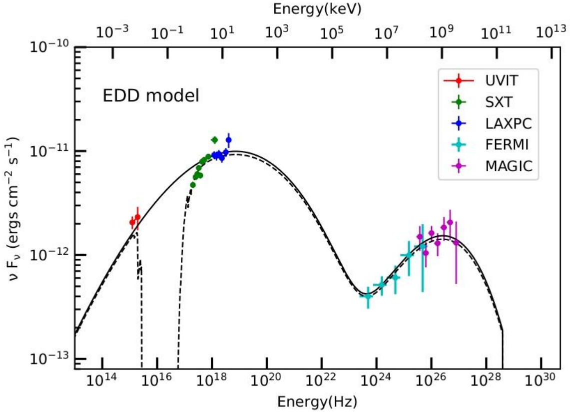

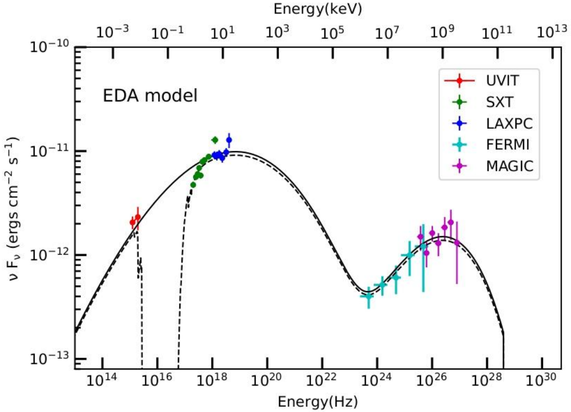

Jet power estimated for all five models

- **The total jet power (P_{jet}):**

$$P_{jet} = 2\pi^2 R^2 \Gamma^2 \beta_c u'_k$$

u'_k are the energy densities in the co-moving jet's frame of the magnetic field, relativistic electrons, and cold protons.

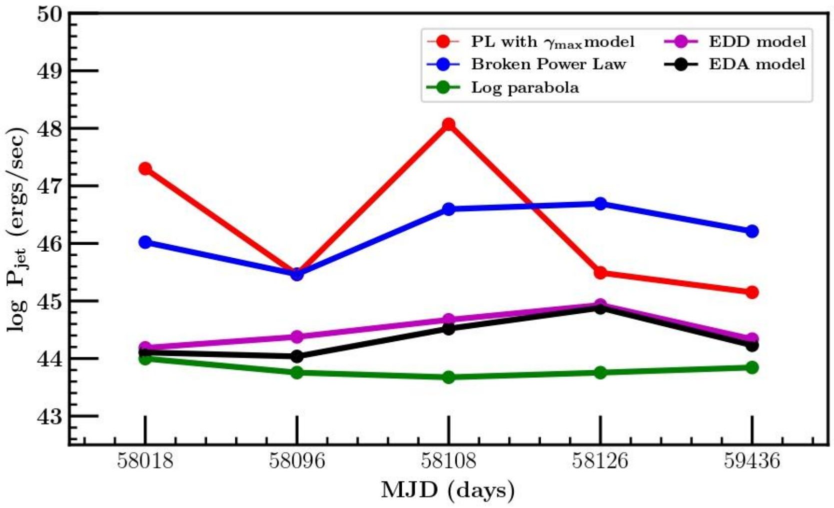

R and Γ values at 10^{17} cm and 20

Jet power estimated for LP & BPL models

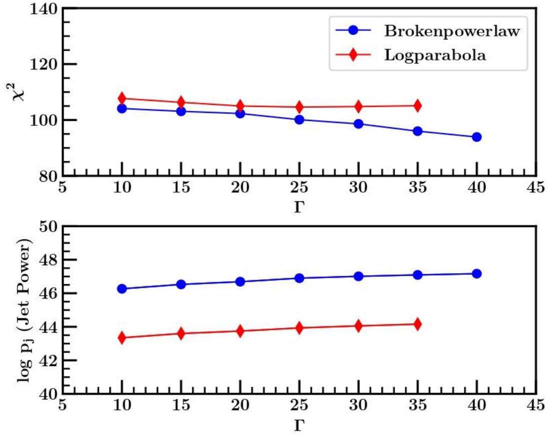

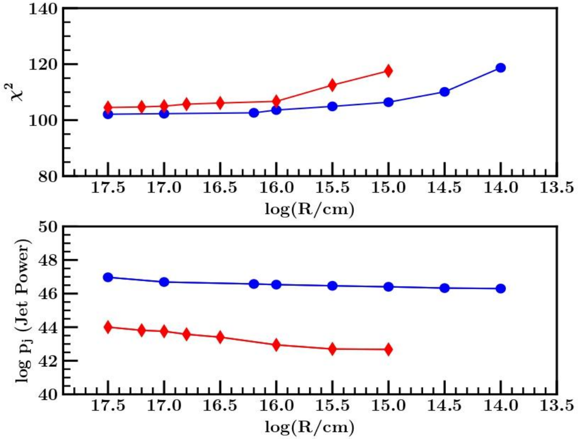

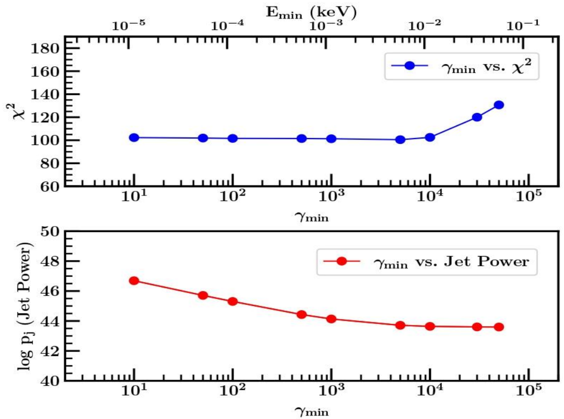

Correlation plots for EDD Model

$$\log_{10}(\psi) = \log_{10}(\eta_R) - \kappa \times \log_{10}(\xi_R)$$

$$\ln(\mathbb{N}) = \frac{\eta_R}{\kappa} A^\kappa + B$$

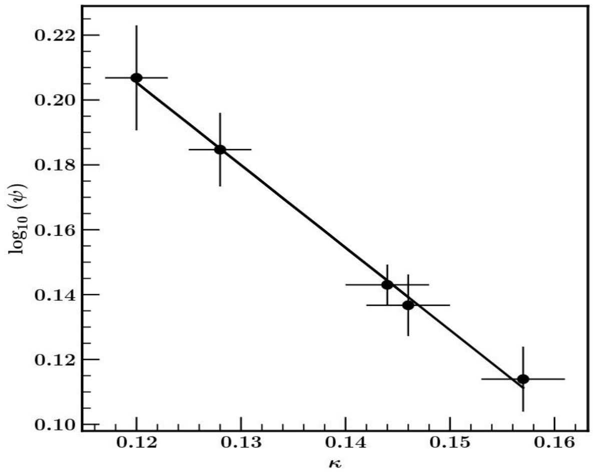

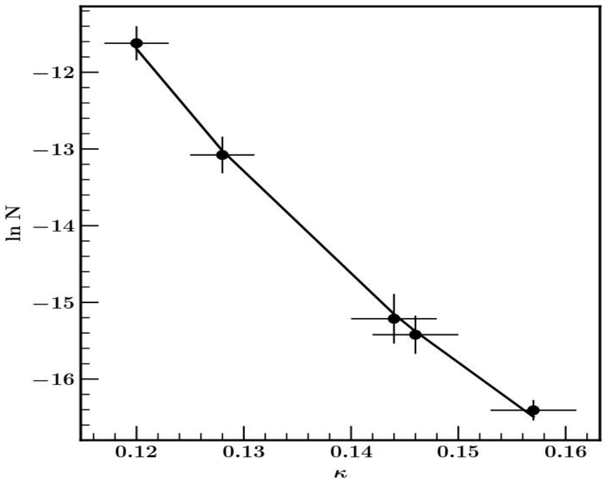

$\log_{10}(\xi_R) = 2.54$, $\log_{10}(\eta_R) = 0.51 \Rightarrow \boldsymbol{\xi_R}^2 = 122$ MeV, $\gamma_R = 3.6 \times 10^8$, and $\eta_R = 3.24$

$A = 9.66 \times 10^{-04}$, $B = -23.4$, $\gamma_0 \sim A\gamma_R \Rightarrow \gamma_0 \sim 3.5 \times 10^5$

Correlation plots for EDA Model

$$\log_{10}(\psi) = \log_{10}(\eta_R) - \kappa \times \log_{10}(\xi_R)$$

$$\ln(\mathbb{N}) = \frac{\eta_R}{\kappa} A^{\kappa} - \kappa \ln(\xi_R) + B$$

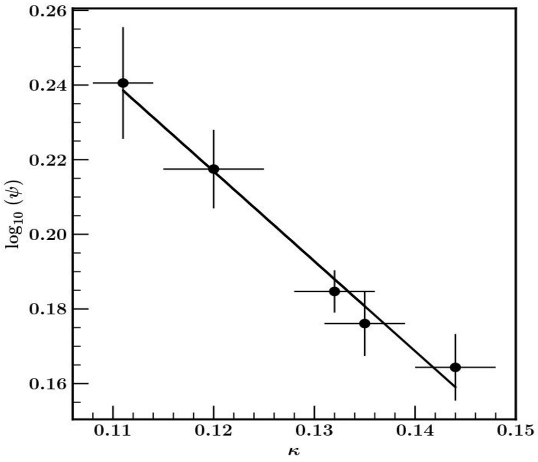

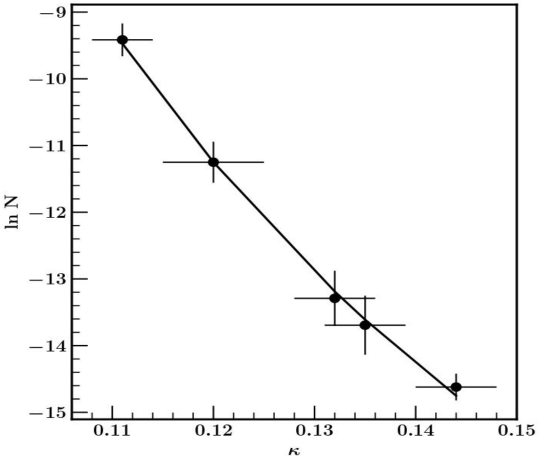

$\xi_R^{\ 2}$ = 66 MeV, γ_R = 2.66 × 10^8, and η_R = 3.21

A = 7.5 × 10^{-04}, B = −21.8, γ_0 ~ 2.0 × 10^5

Summary and conclusions :

- ➢ We conducted broadband SED analysis of 1ES 0229+200 using near-simultaneous observations from September 2017 to August 2021. We applied a one-zone synchrotron and SSC model with different particle distribution models, including log-parabola, broken power law, power law with maximum gamma (γ_{max}), energy-dependent diffusion (EDD), and energy-dependent acceleration (EDA).

- ➢ ***Costamante et al. (2018)*** showed that the broadband SED modeling in hard-TeV blazars can be explained by a one-zone SSC model with a smooth broken power-law distribution. They estimated γ_{break} ~ 10^6 and magnetic fields of a few mG for six hard-TeV blazars. Similarly, in our work on 1ES 0229+200, we also find a magnetic field of a few mG and an electron break energy around ~10^6

- ➢ The jet power for broken power-law and γ-max models, was as high as ~ 10^{47} erg s^{-1} for a minimum lorentz factor γ_{min} = 10 and reduced to ~ 10^{44} erg s^{-1} for γ_{min} = 10^4. For other particle energy distributions with intrinsic curvature, P_{jet} remained around 10^{44} ergs/sec, irrespective of γ_{min}. P_{jet} (≈10^{44} ergs/sec) is only a small fraction of the Eddington luminosity (1.26 ×10^{47} ergs/sec) of the black hole mass (10^9 $M_\odot$), suggesting that accretion processes might be driving the jet.

- ➢ Notably, we found that P_{jet} is nearly independent of both the bulk Lorentz factor (Γ) and the size (R).

Summary and conclusions :

- The compatibility of the spectral fit parameters with the model predictions allows us to calculate ${\xi_R}^2$ = 122 MeV, $\gamma_R = 3.6 \times 10^8$, and $\gamma_0 = 3.5 \times 10^5$ for the EDD model. For the EDA model, these values are ${\xi_R}^2$ = 66 MeV, $\gamma_R = 2.66 \times 10^8$, and $\gamma_0 = 2 \times 10^5$

Thank You !

S.N.	Model Parameters	Unit	epoch-1 21–23 Sep 17	epoch-2 9–10 Dec 17	epoch-3 21–22 Dec 17	epoch-4 8–9 Jan 18	epoch-5 8–12 Aug 21
log-parabola model ($constant * redden * TBabs * eblcor * sscicon * log - parabola$)							
1	α	-	$2.40^{+0.02}_{-0.02}$	$2.65^{+0.02}_{-0.02}$	$2.59^{+0.02}_{-0.02}$	$2.67^{+0.02}_{-0.02}$	$2.44^{+0.02}_{-0.02}$
2	β	-	$0.34^{+0.01}_{-0.01}$	$0.27^{+0.01}_{-0.01}$	$0.29^{+0.01}_{-0.01}$	$0.26^{+0.01}_{-0.01}$	$0.32^{+0.01}_{-0.01}$
3	N	(10^{-11})	$2.39^{+0.2}_{-0.2}$	$1.50^{+0.2}_{-0.2}$	$1.63^{+0.1}_{-0.1}$	$1.42^{+0.2}_{-0.2}$	$1.99^{+0.2}_{-0.2}$
4	B	$(10^{-3}$ G)	$1.02^{+0.1}_{-0.1}$	$2.93^{+0.3}_{-0.3}$	$2.8^{+0.3}_{-0.3}$	$3.04^{+0.5}_{-0.5}$	$1.38^{+0.1}_{-0.1}$
5	$log\ P_{jet}$		$43.9984^{+0.1}_{-0.1}$	$43.7553^{+0.1}_{-0.1}$	$43.6735^{+0.1}_{-0.1}$	$43.7544^{+0.1}_{-0.1}$	$43.8437^{+0.1}_{-0.1}$
6	$\chi^2(dof)$	-	407.2(240)	86.5(88)	138.8(107)	105(106)	151.3(94)
7	$factor_{sxt}$	-	$0.83^{+0.04}_{-0.04}$	$0.76^{+0.02}_{-0.02}$	$0.75^{+0.02}_{-0.02}$	$0.88^{+0.04}_{-0.04}$	$0.63^{+0.03}_{-0.03}$

Broken power law model ($constant * redden * TBabs * eblcor * sscicon * bknpo$)							
1	γ_{min}		10	10	10	10	10
2	γ_{max}		10^8	10^8	10^8	10^8	10^8
3	ξ_{break}	$\sqrt{keV}$	> 10.5	> 6.3	> 10.5	> 7.8	> 5.4
4	p	-	$2.25^{+0.03}_{-0.03}$	$2.46^{+0.03}_{-0.03}$	$2.40^{+0.03}_{-0.03}$	$2.55^{+0.03}_{-0.03}$	$2.32^{+0.01}_{-0.01}$
5	q	-	4.0	4.0	4.0	4.0	4.0
6	N	(10^{-12})	$11.5^{+0.8}_{-0.8}$	$09.10^{+0.6}_{-0.6}$	$10.02^{+0.7}_{-0.7}$	$8.68^{+0.7}_{-0.7}$	$10.7^{+0.9}_{-0.9}$
7	B	$(10^{-3}$ G)	$1.67^{+0.3}_{-0.3}$	$3.12^{+0.3}_{-0.3}$	$2.58^{+0.3}_{-0.3}$	$3.40^{+0.3}_{-0.3}$	$1.97^{+0.3}_{-0.3}$
8	$log\ P_{jet}$		$46.0214^{0.06}_{0.06}$	$45.4643^{0.01}_{0.01}$	$46.5954^{0.01}_{0.01}$	$46.69^{0.01}_{0.01}$	$46.21^{0.008}_{0.008}$
9	$\chi^2(dof)$	-	310(243)	84.8(89)	110.2(108)	102.3(107)	112.4(95)
10	$factor_{sxt}$	-	$1.1^{+0.06}_{-0.06}$	$0.98^{+0.06}_{-0.06}$	$0.90^{+0.06}_{-0.06}$	$1.2^{+0.09}_{-0.09}$	$0.81^{+0.04}_{-0.04}$

S.N.	Model Parameters	Unit	epoch-1 21–23 sep 17	epoch-2 9–10 dec 17	epoch-3 21–22 dec 17	epoch-4 8–9 jan 18	epoch-5 8–12 aug 21
PL with γ_{max} model ($constant * redden * TBabs * eblcor * sscicon * \gamma_{max}$)							
1	p	-	$2.25^{+0.03}_{-0.03}$	$2.51^{+0.01}_{-0.05}$	$2.42^{+0.02}_{-0.09}$	$2.53^{+0.01}_{-0.05}$	$2.30^{+0.03}_{-0.03}$
2	ξ_{max}	-	> 23	> 17	> 31.5	> 8.8	> 13
3	N	10^{-12}	$11.6^{+0.9}_{-0.9}$	$09.01^{+0.24}_{-0.7}$	$9.40^{+0.7}_{-0.7}$	$8.60^{+0.6}_{-0.6}$	$11.3^{+0.8}_{-0.8}$
4	B	10^{-3}G	$1.56^{+0.4}_{-0.4}$	$4.14^{+0.6}_{-0.5}$	$3.68^{+0.6}_{-0.5}$	$4.23^{+0.5}_{-0.5}$	$1.70^{+0.2}_{-0.2}$
5	$log\ P_{jet}$		$47.30^{+0.062}_{-0.062}$	$45.46^{0.067}_{0.067}$	$48.07^{0.069}_{0.069}$	$45.49^{0.07}_{0.07}$	$45.15^{0.07}_{0.07}$
6	$\chi^2(dof)$	-	307.8(243)	82.5(89)	108.2(108)	101.2(107)	111.8(96)
7	$factor_{sxt}$	-	$1.1^{+0.05}_{-0.05}$	$1.01^{+0.05}_{-0.05}$	$0.93^{+0.05}_{-0.05}$	$1.1^{+0.05}_{-0.05}$	$0.83^{+0.05}_{-0.05}$

EDD model ($constant * redden * TBabs * eblcor * sscicon * edd$)

1	B	10^{-3} G	$1.26^{+0.1}_{-0.1}$	$1.44^{+0.3}_{-0.3}$	$2.80^{+0.3}_{-0.3}$	$3.05^{+0.5}_{-0.5}$	$1.27^{+0.1}_{-0.1}$
2	ψ		$1.30^{+0.02}_{-0.02}$	$1.39^{+0.02}_{-0.02}$	$1.53^{+0.04}_{-0.04}$	$1.61^{+0.06}_{-0.06}$	$1.37^{+0.03}_{-0.03}$
3	κ		$0.157^{+0.004}_{-0.004}$	$0.144^{+0.004}_{-0.004}$	$0.128^{+0.003}_{-0.003}$	$0.120^{+0.003}_{-0.003}$	$0.146^{+0.004}_{-0.004}$
4	N	10^{-8}	$7.49^{+1.0}_{-1.0}$	$24.70^{+8.0}_{-8.0}$	$209.0^{+50.0}_{-50.0}$	$897.3^{+200.0}_{-200.0}$	$20.06^{+5.0}_{-5.0}$
5	$log\ P_{jet}$		$44.1847^{+0.007}_{-0.007}$	$44.3757^{+0.01}_{-0.01}$	$44.6721^{+0.1}_{-0.1}$	$44.9290^{+0.1}_{-0.1}$	$44.3367^{+0.008}_{-0.008}$
6	$\chi^2(dof)$		365(242)	80.6(85)	130.5(107)	101.5(106)	137.0(95)
7	$factor_{sxt}$		$0.93^{+0.04}_{-0.04}$	$0.94^{+0.06}_{-0.06}$	$0.74^{+0.04}_{-0.04}$	$0.93^{+0.04}_{-0.04}$	$0.68^{+0.04}_{-0.04}$

EDA model (*constant* ∗ *redden* ∗ *TBabs* ∗ *eblcor* ∗ *sscicon* ∗ *eda*)

1	B	10^{-3} G	$1.26^{+0.1}_{-0.1}$	$1.28^{+0.1}_{-0.1}$	$2.75^{+0.2}_{-0.2}$	$3.15^{+0.2}_{-0.2}$	$1.24^{+0.1}_{-0.1}$
2	κ		$0.144^{+0.004}_{-0.004}$	$0.132^{+0.004}_{-0.004}$	$0.120^{+0.005}_{-0.005}$	$0.111^{+0.003}_{-0.003}$	$0.135^{+0.004}_{-0.004}$
3	ψ		$1.46^{+0.03}_{-0.03}$	$1.53^{+0.02}_{-0.02}$	$1.65^{+0.04}_{-0.04}$	$1.74^{+0.06}_{-0.06}$	$1.50^{+0.03}_{-0.03}$
4	N	10^{-7}	$4.47^{+0.9}_{-0.9}$	$16.90^{+7.0}_{-7.0}$	$130.0^{+40.00}_{-40.00}$	$814.0^{+200.00}_{-200.00}$	$11.30^{+5.0}_{-5.0}$